

New cycloplatinated complexes with 2-arylimidazolines: Synthesis, crystal structures and photophysical properties

Jun-Fang Gong ^{*}, Xin-Heng Fan, Chen Xu, Jin-Lei Li, Yang-Jie Wu ^{*}, Mao-Ping Song

Department of Chemistry, Henan Key Laboratory of Chemical Biology and Organic Chemistry, Key Laboratory of Applied Chemistry of Henan Universities, Zhengzhou University, Zhengzhou 450052, PR China

Received 8 December 2006; received in revised form 30 December 2006; accepted 9 January 2007

Available online 30 January 2007

Abstract

The synthesis, crystal structures and photophysical properties of a series of cycloplatinated complexes are presented. The complexes have the general formula $(C^{\wedge}N)Pt(O^{\wedge}O)$, where $O^{\wedge}O$ is acetylacetonate and $C^{\wedge}N$ represents 2-arylimidazoline ligands. All of them are luminescent in CH_2Cl_2 solution at room temperature. Different aryl group on N-1 of the ligand has no significant effect on the emission properties of the platinum complexes. While introducing alkyl group on N-1 or electron-donating group on 2-aryl ring does result in a blue shift of emission maxima or even an increase in emission intensity.

© 2007 Elsevier B.V. All rights reserved.

Keywords: Cycloplatinated; 2-Arylimidazolines; Crystal structures; Photoluminescent

1. Introduction

Square-planar platinum complexes have received considerable attention due to their intriguing photophysical and photochemical properties [1]. In particular, cyclometalated platinum complexes with pyridines such as 2-arylpyridine [2], 6-phenyl-2,2'-bipyridine [3], 1,3-di(2-pyridyl)benzene [4] and other cyclometalating ligands [5] have been extensively investigated over the past years. These luminescent complexes are an attractive class of molecules as potential phosphorescent emitters in organic light-emitting devices (OLEDs) because the strong spin-orbit coupling of the heavy platinum atom allows for efficient intersystem crossing (ISC) from the singlet (S_1) to the triplet (T_n) as well as the enhancement of the T_1-S_0 transition. Thus, OLEDs based on these phosphors can utilize all of the electrogenerated singlet and triplet excitons, theoretically attaining an internal quantum efficiency of

100%. Furthermore, the emission color of cyclometalated platinum complexes can be tuned through rational modification of the cyclometalating ligand or ancillary ligand [2]. In search of new LED emitters, we synthesized a series of cycloplatinated complexes with 2-arylimidazolines (Scheme 1). The reason for the choice of 2-arylimidazoline as cyclometalating ligand is that it can be easily modified by changing the substituent on N-1 or 2-aryl group. Some related palladacyclic complexes and a chloro-bridged platinacyclic dimer derived from 2-phenylimidazoline (**1c**) have been previously reported and their *in vitro* antileukaemic activity has been investigated [6]. Herein we wish to present our results on the synthesis, crystal structures and photophysical properties of new platinacyclic complexes **3a–3e**.

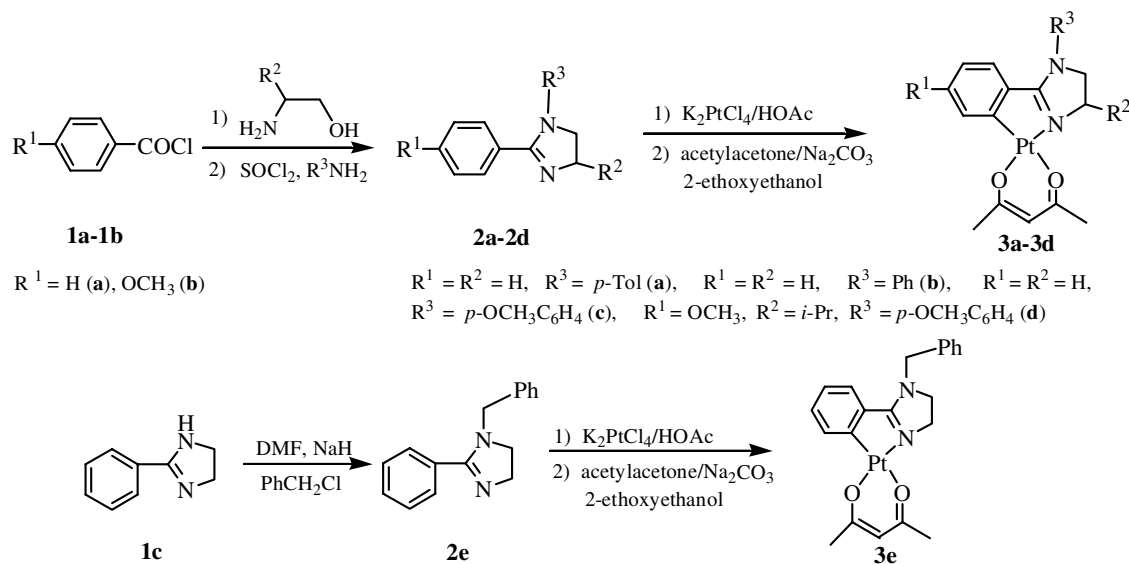
2. Results and discussion

2.1. Synthesis and characterization

The synthesis of 2-arylimidazolines **2a–2e** and the corresponding cyclometalated platinum (II) complexes **3a–3e** is shown in Scheme 1. Ligands **2a–2d** were prepared from benzoyl chloride or *p*-methoxybenzoyl chloride in two steps

^{*} Corresponding authors. Tel.: +86 371 67763207; fax: +86 371 67766667 (Jun-Fang Gong).

E-mail addresses: gongjf@zzu.edu.cn (J.-F. Gong), wj@zzu.edu.cn (Y.-J. Wu).



Scheme 1.

according to the published procedure [7]. The reaction of **1a** or **1b** with aminoethanol or valinol in the presence of Et_3N in THF at room temperature afforded the amido alcohols, which were treated with excess thionyl chloride, followed by arylamines such as *p*-toluidine or phenylamine or *p*-methoxyaniline. After basic workup with 10% NaOH and purification by preparative TLC on silica gel plates eluting with ethyl acetate, 2-arylimidazolines **2a–2d** were obtained. Ligand **2e** was synthesized from the reaction of 2-phenylimidazoline (**1c**) with benzylchloride in the presence of NaH base. Then treatment of K_2PtCl_4 with 2 equiv of ligand **2** produced the proposed chloro-bridged dimer [2a,2b], which was subsequently converted into the expected cycloplatinated complexes **3** upon reaction with acetylacetonate (acac) in the presence of Na_2CO_3 in 2-ethoxyethanol. Complexes **3** were isolated as air-stable yellow solids in 20–33% yields. All the new compounds were well characterized by 1H NMR, ^{13}C NMR, ESI-MS, IR and

elemental analysis. Furthermore, the molecular structures of both **3c** and **3d** were determined by X-ray single crystal analysis.

The molecular structures of complexes **3c** and **3d** are shown in Figs. 1 and 3 (displacement ellipsoids are drawn at the 30% probability level). Crystallographic and data collection parameters are summarized in Table 1. Selected bond lengths (Å) and angles (°) are given in Table 2. The Pt atom in each complex is in a slightly distorted square-planar environment bonded to the nitrogen and the C1(C6) atoms of 2-arylimidazoline ligand, the two oxygen atoms of acac. The deviations of the Pt atoms from the planes for complexes **3c** and **3d** are 0.0376 Å and 0.0149 Å, respectively. In two complexes, the arylimidazoline metallacycle is essentially flat. While the N-aryl ring is not coplanar with the plane of the (arylimidazoline)Pt(acac) fragment and the dihedral angles between them are 88.1° and 87.0° for complexes **3c** and **3d**, respectively. These characters are similar

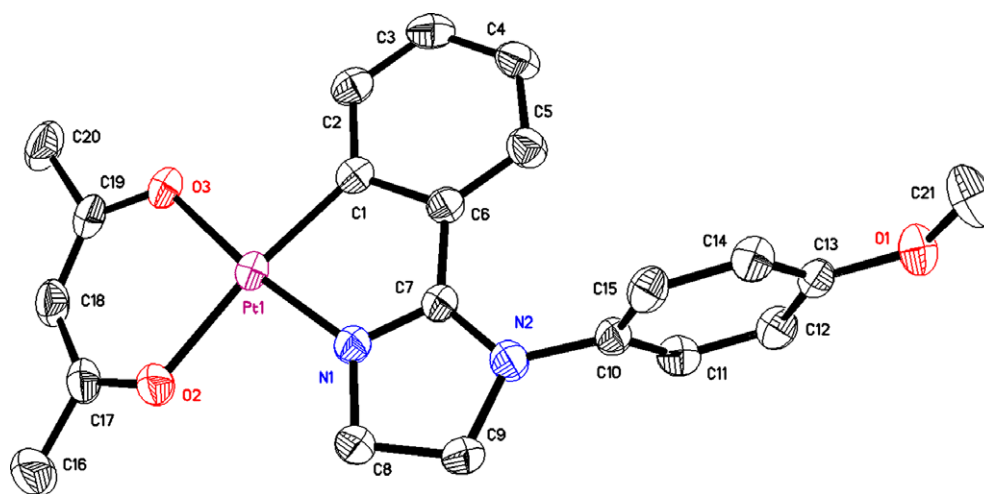
Fig. 1. Molecular structure of complex **3c**. Hydrogen atoms are omitted for clarity.

Table 1
Crystallographic and data collection parameters for **3c** and **3d**

Empirical formula	C ₂₁ H ₂₂ N ₂ O ₃ Pt	C ₂₅ H ₃₀ N ₂ O ₄ Pt
Formula weight	545.50	617.60
Temperature (K)	291(2)	293(2)
Wavelength (Å)	0.71073	0.71073
Crystal system	Monoclinic	Monoclinic
Space group	P2(1)/n	P2(1)/n
Unit cell dimensions		
<i>a</i> (Å)	8.777(8)	10.016(2)
<i>b</i> (Å)	18.944(16)	24.022(5)
<i>c</i> (Å)	12.726(11)	10.334(2)
α (°)	90	90
β (°)	106.349(10)	90.17(3)
γ (°)	90	90
Volume (Å ³)	2030.5(3)	2486.5(9)
Z	4	4
Calculated density (Mg/m ³)	1.784	1.650
Absorption coefficient (mm ⁻¹)	6.933	5.675
<i>F</i> (000)	1056	1216
Crystal size (mm)	0.41 × 0.15 × 0.07	0.20 × 0.18 × 0.14
Theta range for data collection	2.65–27.50°	2.15–25.50°
Index ranges	–11 ≤ <i>h</i> ≤ 11, –24 ≤ <i>k</i> ≤ 24, –16 ≤ <i>l</i> ≤ 16	–11 ≤ <i>h</i> ≤ 11, –29 ≤ <i>k</i> ≤ 29, –12 ≤ <i>l</i> ≤ 0
Reflections collected/unique (<i>R</i> _{int})	17771/4664 (0.0285)	7695/4349 (0.0749)
Completeness to 2 θ	99.8%	93.9%
Maximum and minimum transmission	0.6280 and 0.1647	0.5038 and 0.3965
Refinement method	Full-matrix least-squares on <i>F</i> ²	Full-matrix least-squares on <i>F</i> ²
Data/restraints/parameters	4664/0/247	4349/0/290
Goodness-of-fit on <i>F</i> ²	1.030	1.072
Final <i>R</i> indices [<i>I</i> > 2 σ (<i>I</i>)]	<i>R</i> ₁ = 0.0226, <i>wR</i> ₂ = 0.0487	<i>R</i> ₁ = 0.0588, <i>wR</i> ₂ = 0.1557
<i>R</i> indices (all data)	<i>R</i> ₁ = 0.0323, <i>wR</i> ₂ = 0.0526	<i>R</i> ₁ = 0.0715, <i>wR</i> ₂ = 0.1645
Largest difference in peak and hole (e Å ⁻³)	0.302 and –1.196	1.046 and –1.031

Table 2
Selected bond lengths (Å) and angles (°) for **3c** and **3d**

Compound	3c	3d
Pt(1)–N(1)	1.980(3)	1.980(10)
Pt(1)–C(1)/Pt(1)–C(6)	1.976(3)	1.989(11)
Pt(1)–O(2)/Pt(1)–O(1)	2.095(2)	2.093(8)
Pt(1)–O(3)/Pt(1)–O(2)	2.018(2)	2.018(8)
C(1)–Pt(1)–N(1)/C(6)–Pt(1)–N(1)	80.59(11)	80.6(4)
C(1)–Pt(1)–O(3)/C(6)–Pt(1)–O(2)	93.03(11)	94.3(4)
N(1)–Pt(1)–O(3)/N(1)–Pt(1)–O(2)	173.61(9)	174.8(3)
C(1)–Pt(1)–O(2)/C(6)–Pt(1)–O(1)	173.02(10)	173.9(4)
N(1)–Pt(1)–O(2)/N(1)–Pt(1)–O(1)	94.00(9)	93.4(3)
O(3)–Pt(1)–O(2)/O(2)–Pt(1)–O(1)	92.38(9)	91.7(3)
C(17)–O(2)–Pt(1)/C(2)–O(1)–Pt(1)	122.4(2)	122.9(7)
C(19)–O(3)–Pt(1)/C(4)–O(2)–Pt(1)	123.5(2)	124.1(8)
C(7)–N(1)–Pt(1)/C(12)–N(1)–Pt(1)	117.0(2)	116.9(7)
C(8)–N(1)–Pt(1)/C(20)–N(1)–Pt(1)	133.2(2)	131.5(6)
C(2)–C(1)–Pt(1)/C(7)–C(6)–Pt(1)	128.5(2)	127.0(8)
C(6)–C(1)–Pt(1)/C(11)–C(6)–Pt(1)	115.1(2)	114.6(7)

to those in the chiral pincer Pt(II) complexes with 1,3-bis(2'-imidazolyl)phenyl which have been previously reported by us [8]. All the bond lengths and angles around Pt(II) in **3c** and **3d** are essentially identical and the data are also comparable to those found in the related cycloplatinated complexes [2a,2b]. The two Pt–O bond lengths in **3c** or **3d** are different with the longer distances corresponding to oxygen *trans* to the cyclometalating carbon. It is

found that the Pt–C bond lengths (1.976(3) Å for **3c** and 1.989(11) Å for **3d**) are slightly longer, while the Pt–N bond lengths (1.980(3) Å for **3c** and 1.980(10) Å for **3d**) are slightly shorter in comparison with the corresponding bond lengths for the bis(imidazoline) pincer Pt(II) complex (1.910(11) or 1.957(13) Å for Pt–C, and 2.008–2.043 for Pt–N) [8].

Fig. 2 shows that in the crystal of **3c** there exist three types of intermolecular Pt...H hydrogen bonds (PtA...H2OZ = 3.216 Å, Pt1Z...H9A = 3.011 Å, Pt1Z...H11A = 3.121 Å), which are attributed to construct the 1D chain structure of complex **3c**. In addition, hydrogen bonds between oxygen atom and the adjacent C–H group of benzene ring are present in the crystal (the distance is 2.532 Å), which lead to the generation of the 2D supermolecular architecture. Fig. 4 shows that complex **3d** has a one-dimensional zigzag chain structure formed by Pt...H (Pt1C...H14 = 3.133 Å, Pt...H17 = 3.176 Å) hydrogen bonds. Molecules of **3c** are found to pack in a head-to-head fashion. While those of **3d** are in a head-to-tail fashion. The Pt...Pt distances between adjacent complexes are 6.647 Å in **3c**, 8.215 Å and 9.905 Å in **3d**, indicating a lack of d⁸–d⁸ interaction [2a,5b,9]. The two adjacent ligand planes in **3c** are not parallel (dihedral angle of 25.5°) with an interplanar distance of 4.2314 Å, which is too long for a π – π stacking interaction [2b,10]. While those in **3d** are parallel with corresponding interplanar distances of ca. 4.4451 Å and 5.2156 Å, respectively.

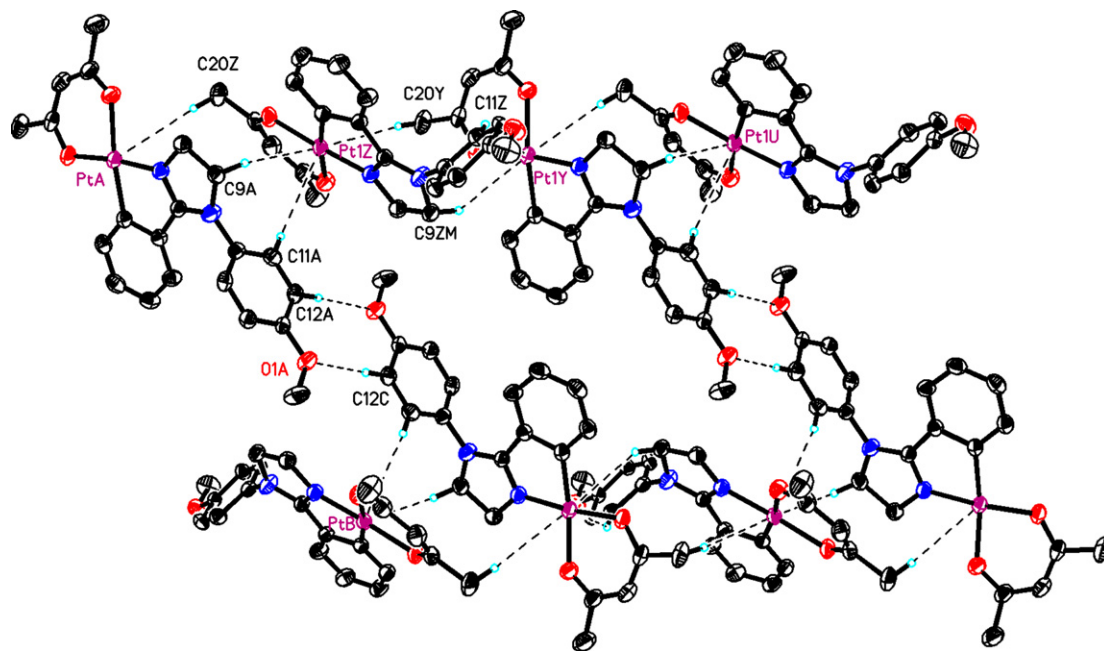


Fig. 2. Two-dimensional lamellar structure of complex 3c showing the hydrogen bonds. Non-hydrogen bonding H atoms are omitted for clarity.

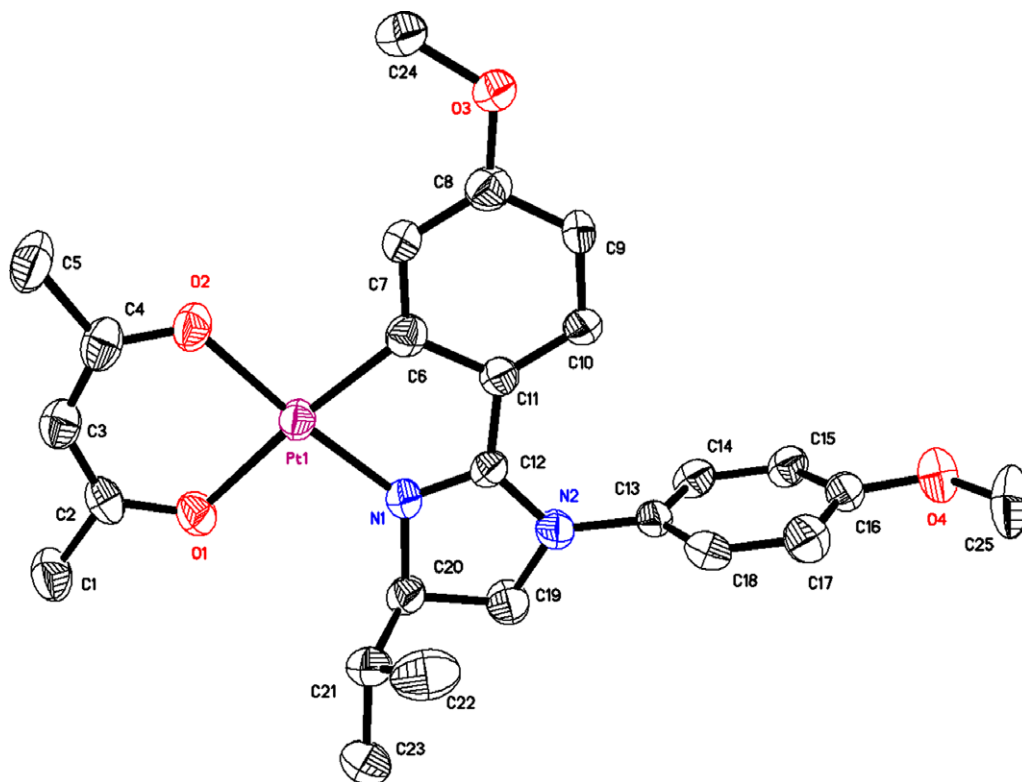


Fig. 3. Molecular structure of complex 3d. Hydrogen atoms are omitted for clarity.

2.2. Photophysical properties of the cyclometalated complexes

The absorption spectra data and emission data of the ligands **2** and complexes **3** are summarized in Table 3. All the UV–vis spectra of complexes **3** in CH_2Cl_2 have sim-

ilar features. The intense absorption bands at wavelengths below 300 nm are attributed to $\pi\text{-}\pi^*$ transitions of the ligands. In addition, all of the complexes have a broad, less intense absorption band at λ_{max} 347–364 nm, which tails beyond 400 nm. It can tentatively be assigned to MLCT transition resulting from the promotion of an electron from

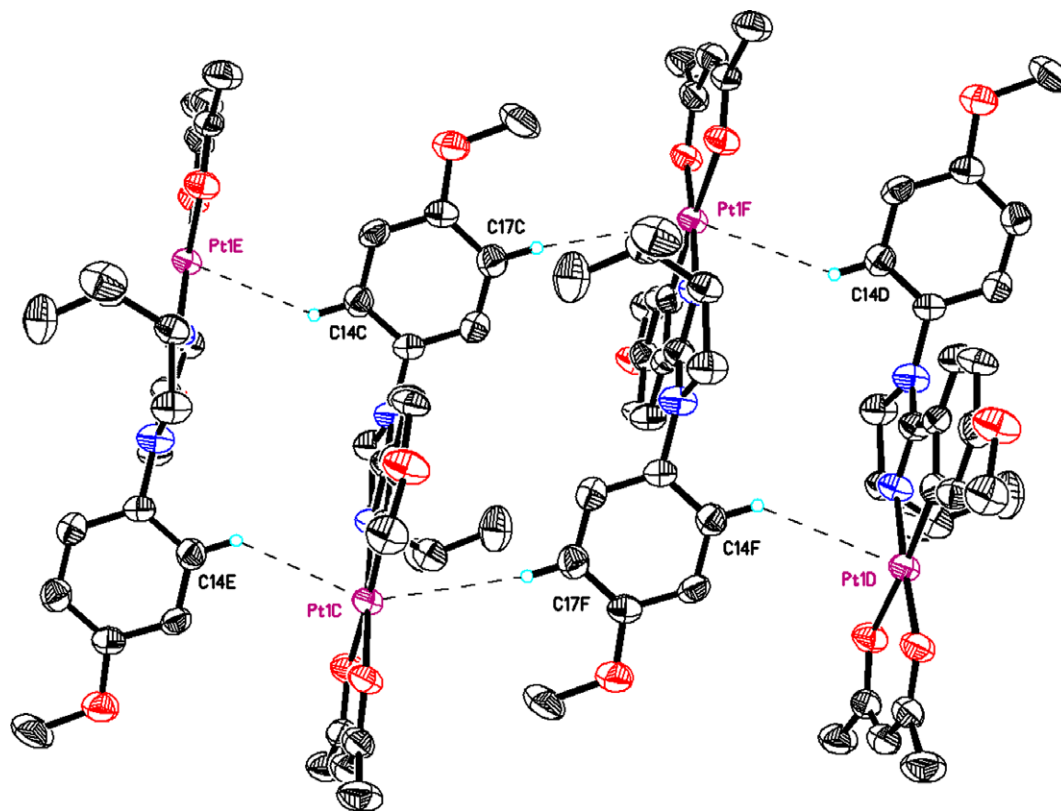


Fig. 4. One-dimensional zigzag chain structure of complex **3d** showing the hydrogen bonds. Non-hydrogen bonding H atoms are omitted for clarity.

Table 3
Photophysical properties of **2** and **3**

Compounds	λ_{\max}^a /nm (ϵ^b ($M^{-1} \text{cm}^{-1}$))	λ_{ex}^c (nm)	λ_{em}^d (nm)	Φ^e (%)
2a	229 (14490)	289	368	
2b	228 (12160)	299	370	
2c	230 (19302)	330	482	
2d	228 (13066), 279 (12215)	324	465	
2e	230 (10356)	292	344, 406	
3a	229 (18603), 244 sh (17082), 363 (7556)	409	562, 594	1.67
3b	229 (17277), 244 (16398), 364 (7188)	411	560, 599	2.62
3c	228 (28957), 243 sh (23787), 363 (10060)	418	564, 588	2.30
3d	228 (24243), 248 (22968), 347 (9827)	411	539, 560	3.49
3e	230 (20236), 244 (19782), 362 (6530)	398	538, 574	3.03

^a Absorption maxima in CH_2Cl_2 solution at room temperature.

^b Molecular absorption coefficient.

^c Excitation maximum in $5 \times 10^{-4} \text{M}$ CH_2Cl_2 solution at room temperature.

^d Emission maximum in $5 \times 10^{-4} \text{M}$ CH_2Cl_2 solution at room temperature.

^e Quantum yield obtained from measurements using quinine sulfate in 1 M H_2SO_4 ($\Phi = 0.546$) as standard [11].

Pt(d) HOMO to the π^* LUMO on the 2-arylimidazole ligand. The change of the substituent on N-1 of the ligand from C_6H_5 (**3b**) to $p\text{-CH}_3\text{C}_6\text{H}_4$ (**3a**) or $p\text{-OCH}_3\text{C}_6\text{H}_4$ (**3c**) or even $\text{CH}_2\text{C}_6\text{H}_5$ (**3e**) has very little effect on the position of this band (λ_{\max} around 363 nm), if any. However, this absorption is slightly blue-shifted for complex **3d** (λ_{\max} 347 nm) with electron-donating group (OMe) on 2-aryl ring. Compared with those for the bis(imidazoline) pincer Pt(II) complexes (λ_{\max} around 390 nm), all the lowest energy MLCT absorption bands for complexes **3** are blue-shifted [8].

It is found that the substituents on N-1 greatly influence the fluorescent emission properties of ligands **2** in CH_2Cl_2 solution at room temperature. Thus, changing the substituent from $p\text{-CH}_3\text{C}_6\text{H}_4$ (**2a**) or C_6H_5 (**2b**) to more electron-donating aryl group such as $p\text{-OCH}_3\text{C}_6\text{H}_4$ (**2c** or **2d**) leads to an obvious red shift of the emission maximum (368 nm and 370 nm *vs* 482 and 465 nm) and a significant increase in emission intensity. For ligand **2e** with CH_2Ph on N-1, it displays emissions at 344 and 406 nm with similar intensity to that of **2a** and **2b**. Upon photoexcitation, all the platinum complexes studied also show emission in CH_2Cl_2

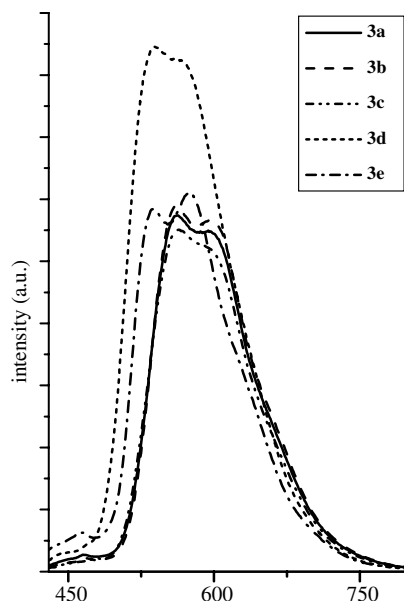


Fig. 5. Emission spectra of complexes **3** in 5×10^{-4} M CH_2Cl_2 solution at room temperature.

solution at room temperature. Different from the substituent effects in ligands **2**, the change of the substituent on N-1 from *p*- $\text{CH}_3\text{C}_6\text{H}_4$ (**3a**) or C_6H_5 (**3b**) to *p*- $\text{OCH}_3\text{C}_6\text{H}_4$ (**3c**) has no significant effect on the room-temperature emission properties of the complexes and these three compounds show very similar spectra to one another, with emission maxima around 560 and 590 nm (Fig. 5). A possible reason for the result is that the N-aryl is unconjugated with the other parts of the complex which is confirmed by X-ray single crystal analysis of **3c** and **3d**. The related pincer Pt (II) complexes display broad structureless emissions with λ_{max} at 575–577 nm [8]. On the other hand, the emission peaks of complex **3d** with a methoxy group on 2-aryl ring and **3e** with CH_2Ph on N-1 are subject to a small blue shift. For **3d**, the emission intensity also increases. The above results give some useful information on further ligand modification for tuning the emission properties of the related platinum complexes. Finally, it is found that the emission maxima of these complexes are significantly red-shifted compared with the value of 486 nm reported for [(2-phenylpyridine)Pt(acac)] at room temperature in 2-MeTHF [2a].

In summary, a series of cycloplatinated complexes with 2-arylimidazolines have been synthesized and characterized. All the complexes display photoluminescence in CH_2Cl_2 solution at room temperature. Although the substituents on N-1 greatly influence the fluorescent emission properties of 2-arylimidazoline ligands, the different aryl group on N-1 has no significant effect on the emission properties of the platinum complexes. Introducing alkyl group on N-1 or electron-donating group on 2-aryl ring does result in a blue shift of emission maxima or even an increase in emission intensity. Further studies are in progress.

3. Experimental

3.1. General

All reactions were carried out under a dry nitrogen atmosphere using standard Schlenk techniques. Compounds **1b** [12] and **1c** [13] were prepared according to literature methods. All the other reagents were used as commercial sources. Melting points were measured using a WC-1 microscopic apparatus and were uncorrected. Elemental analysis was determined with a Thermo Flash EA 1112 elemental analyzer. IR spectra were collected on a Bruker VECTOR22 spectrophotometer in KBr pellets. ^1H and ^{13}C NMR spectra were recorded on a Bruker DPX-400 spectrometer in CDCl_3 with TMS as an internal standard. Mass spectra were performed on the Agilent LC/MSD Trap XCT instrument. UV–Vis absorption spectra were recorded using a Perkin Elmer Lambda 35 spectrometer at room temperature. The photoluminescence spectra were measured on a HORIBA Jobin Yvon FluoroMax-P spectrofluorimeter at room temperature.

3.2. Synthesis of ligands 2a–2e

3.2.1. General procedure for the synthesis of ligands 2a–2d

To a stirred solution of amino alcohol (7.5 mmol) and Et_3N (2.10 mL, 15 mmol) in THF (10 mL) was added dropwise a solution of benzoyl chloride (0.58 mL, 5 mmol) or *p*-methoxy-benzoyl chloride (0.68 mL, 5 mmol) in 60 mL THF at room temperature. After stirring for 16 h, the reaction mixture was filtered and evaporated. The residue was purified by passing through a short silica gel column with acetone/petroleum ether (1:1) as eluent, giving white solids of the corresponding amido alcohol. Then the obtained amido alcohol (2.4 mmol) reacted with thionyl chloride (0.71 mL, 9.7 mmol) at reflux for 6 h. Excess thionyl chloride was evaporated. The residue was dissolved in dry diethyl ether (5 mL) and filtered to remove insoluble impurities. To this solution was added dry triethylamine (1 mL, 7.2 mmol), followed by *p*-toluidine, or phenylamine or *p*-methoxyaniline (2.64 mmol). After stirring for 5 h at room temperature, 10% NaOH (10 mL) was added and stirred for 24 h. The aqueous was extracted with dichloro-methane and the organic layer was dried over MgSO_4 and evaporated. The crude was purified by preparative TLC on silica gel plates eluting with ethyl acetate to afford ligands **2a–2d** as pale yellow oil (which will solidify during preservation). **2a–2c** are known compounds.

Characterization data for **2d**: 56.5% yield. IR (KBr, cm^{-1}): 1613 ($\nu_{\text{C}=\text{N}}$). ^1H NMR (400 MHz, CDCl_3): δ 0.95 (d, $J = 6.7$ Hz, 3H, $\text{CH}(\text{CH}_3)_2$), 1.03 (d, $J = 6.7$ Hz, 3H, $\text{CH}(\text{CH}_3)_2$), 1.89–1.93 (m, 1H, CHMe_2), 3.51–3.58 (m, 1H, CH_2), 3.73 (s, 3H, OCH_3), 3.76 (s, 3H, OCH_3), 3.98–4.04 (m, 2H, $\text{CH}_2 + \text{NCH}$), 6.70–6.78 (m, 6H, ArH), 7.43 (d, $J = 8.6$ Hz, 2H, ArH); ^{13}C NMR (100 MHz, CDCl_3): δ 17.8, 18.9, 33.2, 55.2, 55.4, 57.2, 69.9, 113.3, 114.0, 123.5, 125.0, 130.4, 137.2, 156.0, 160.6, 161.6. ESI-MS

(M+H)⁺ Calc. for C₂₀H₂₅N₂O₂: 325.2, found: 325.1. Anal. Calc. for C₂₀H₂₄N₂O₂: C, 74.04; H, 7.46; N, 8.64. Found: C, 74.19; H, 7.54; N, 8.53%.

3.2.2. Synthesis of **2e**

A 50 mL three neck round-bottom flask was equipped with a 10 mL addition funnel and a nitrogen inlet. To a stirring solution of sodium hydride (72 mg, 3 mmol) in DMF (5.0 mL) was added dropwise a solution of 2-phenylimidazoline (300 mg, 2 mmol) in DMF (5.0 mL) at 0 °C. After 30 min, the resulting solution was added dropwise a solution of benzyl chloride (0.36 mL, 3 mmol) in DMF (5.0 mL) at room temperature. After stirring for 24 h at room temperature, the reaction was poured into 300 mL of water and extracted with chloroform. The combined organic phases were washed with brine, and then dried over magnesium sulfate. After filtering and concentrating, the residue was applied to a column of silica gel with chloroform/methanol (5:1) as eluent to give **2e** as an oil. **2e** is also a known compound.

3.3. General procedure for the synthesis of cycloplatinated complexes **3a–3e**

A mixture of 2-arylimidazoline ligand (0.4 mmol) and K₂PtCl₄ (83 mg, 0.2 mmol) in HOAc (4 mL) were refluxed for 30 h. The reaction mixture was allowed to cool down to room temperature and filtered. The obtained yellow precipitate was thought to be the chloro-bridged dimer which was washed with HOAc, H₂O and acetone, respectively, then dried in vacuum. Without further purification and characterization, the dimer was treated with 3 equiv of acetylacetone in the presence of 10 equiv of Na₂CO₃ in 2-ethoxyethanol at 100 °C under nitrogen for 24 h. After the removal of the solvent, the residue was purified by preparative TLC on silica gel plates using CH₂Cl₂ as the eluent to afford **3**.

3a: Yellow solid, 20.5% yield. m.p.: 212–214 °C. IR (KBr, cm⁻¹): 1567 (ν_{C=N} and ν_{C=O}). ¹H NMR (400 MHz, CDCl₃): δ 1.90 (s, 3H, CH₃), 1.94 (s, 3H, CH₃), 2.41 (s, 3H, CH₃), 3.96–4.01 (m, 2H, CH₂), 4.09–4.14 (m, 2H, CH₂), 5.43 (s, 1H, CH), 6.45 (d, *J* = 7.7 Hz, 1H, ArH), 6.69 (app t, 1H, *J* = 7.5 Hz, ArH), 7.07 (app t, *J* = 7.5 Hz, 1H, ArH), 7.17 (d, *J* = 8.3 Hz, 2H, ArH), 7.22 (d, *J* = 8.3 Hz, 2H, ArH), 7.58 (d, *J* = 7.5 Hz, 1H, ArH); ¹³C NMR (100 MHz, CDCl₃): δ 21.2, 27.3, 27.9, 48.7, 55.6, 102.2, 121.9, 126.1, 126.3, 130.1, 130.3, 130.6, 134.9, 137.5, 138.5, 140.1, 175.6, 183.1, 184.9. ESI-MS: (M+H)⁺ Calc. for C₂₁H₂₃N₂O₂Pt: 530.1, found: 530.3. Anal. Calc. for C₂₁H₂₂N₂O₂Pt: C, 47.64; H, 4.19; N, 5.29. Found: C, 47.93; H, 4.29; N, 5.19%.

3b: Yellow solid, 21.4% yield. m.p.: 179–181 °C. IR (KBr, cm⁻¹): 1570 (ν_{C=N} and ν_{C=O}). ¹H NMR (400 MHz, CDCl₃): δ 1.91 (s, 3H, CH₃), 1.95 (s, 3H, CH₃), 3.98–4.03 (m, 2H, CH₂), 4.13–4.18 (m, 2H, CH₂), 5.43 (s, 1H, CH), 6.47 (d, *J* = 7.4 Hz, 1H, ArH), 6.69 (app t, 1H, *J* = 7.5 Hz, ArH), 7.07 (app t, *J* = 7.5 Hz,

1H, ArH), 7.28–7.36 (m, 3H, PhH), 7.41–7.44 (m, 2H, PhH), 7.58 (d, *J* = 7.5 Hz, 1H, ArH); ¹³C NMR (100 MHz, CDCl₃): δ 27.3, 27.9, 48.8, 55.4, 102.2, 121.9, 126.1, 126.2, 127.4, 129.7, 130.1, 130.6, 134.8, 140.2, 141.2, 175.5, 183.2, 184.9. ESI-MS (M+H)⁺ Calc. for C₂₀H₂₁N₂O₂Pt: 516.1, found: 516.1. Anal. Calc. for C₂₀H₂₀N₂O₂Pt: C, 46.60; H, 3.91; N, 5.43. Found: C, 46.86; H, 4.02; N, 5.28%.

3c: Yellow solid, 33.2% yield. m.p.: 199–200 °C. IR (KBr, cm⁻¹): 1567 (ν_{C=N} and ν_{C=O}). ¹H NMR (400 MHz, CDCl₃): δ 1.90 (s, 3H, CH₃), 1.94 (s, 3H, CH₃), 3.85 (s, 3H, OCH₃), 3.95–4.00 (m, 2H, CH₂), 4.06–4.11 (m, 2H, CH₂), 5.43 (s, 1H, CH), 6.37 (d, *J* = 7.8 Hz, 1H, ArH), 6.66–6.70 (m, 1H, ArH), 6.94 (d, *J* = 8.8 Hz, 2H, ArH), 7.05–7.08 (m, 1H, ArH), 7.22 (d, *J* = 8.8 Hz, 2H, ArH), 7.57 (d, *J* = 7.6 Hz, 1H, ArH); ¹³C NMR (100 MHz, CDCl₃): δ 27.3, 27.9, 48.7, 55.5, 55.8, 102.2, 114.9, 122.0, 126.0, 128.1, 130.0, 130.6, 133.8, 134.9, 140.1, 158.9, 175.8, 183.1, 184.9. ESI-MS: (M+H)⁺ Calc. for C₂₁H₂₃N₂O₃Pt: 546.1, found: 546.3. Anal. Calc. for C₂₁H₂₂N₂O₃Pt: C, 46.24; H, 4.07; N, 5.14%. Found: C, 46.52; H, 4.10; N, 5.05%.

3d: Yellow solid, 20.3% yield. m.p.: 186–188 °C. IR (KBr, cm⁻¹): 1575 (ν_{C=N} and ν_{C=O}). ¹H NMR (400 MHz, CDCl₃): δ 0.90–0.92 (m, 6H, CH(CH₃)₂), 1.87 (s, 3H, CH₃), 1.92 (s, 3H, CH₃), 2.61–2.65 (m, 1H, CHMe₂), 3.79–3.82 (m, 1H, CH₂), 3.80 (s, overlapped with CH₂, 3H, OCH₃), 3.84 (s, 3H, OCH₃), 4.05–4.10 (m, 1H, CH₂), 4.12–4.17 (m, 1H, NCH), 5.41 (s, 1H, CH), 6.25 (dd, *J* = 2.6, 8.6 Hz, 1H, ArH), 6.33 (d, *J* = 8.6 Hz, 1H, ArH), 6.92–6.95 (m, 2H, ArH), 7.12 (d, *J* = 2.6 Hz, 1H, ArH), 7.15–7.19 (m, 2H, ArH); ¹³C NMR (100 MHz, CDCl₃): δ 14.3, 18.5, 27.3, 27.9, 29.3, 55.0, 55.1, 55.5, 64.8, 102.0, 108.4, 114.2, 114.8, 127.2, 127.4, 127.9, 133.8, 142.4, 158.7, 160.5, 173.6, 183.1, 184.6. ESI-MS: (M+H)⁺ Calc. for C₂₅H₃₁N₂O₄Pt: 618.2, found: 618.7. Anal. Calc. for C₂₅H₃₀N₂O₄Pt: C, 48.62; H, 4.90; N, 4.54. Found: C, 48.84; H, 5.01; N, 4.49%.

3e: Yellow solid, 20.6% yield. m.p.: 155–157 °C. IR (KBr, cm⁻¹): 1569 (ν_{C=N} and ν_{C=O}). ¹H NMR (400 MHz, CDCl₃): δ 1.88 (s, 3H, CH₃), 1.94 (s, 3H, CH₃), 3.73–3.78 (m, 2H, CH₂), 3.83–3.89 (m, 2H, CH₂), 4.92 (s, 2H, CH₂Ph), 5.41 (s, 1H, CH), 6.91 (t, *J* = 7.5 Hz, 1H, ArH), 7.15 (t, *J* = 7.5 Hz, 1H, ArH), 7.25–7.38 (m, 6H, PhH + ArH), 7.65 (d, *J* = 7.6 Hz, 1H, ArH); ¹³C NMR (100 MHz, CDCl₃): δ 27.3, 27.9, 29.7, 48.3, 51.6, 102.2, 122.5, 124.8, 126.9, 127.9, 129.0, 130.2, 131.2, 135.0, 136.4, 140.5, 183.2, 184.9. ESI-MS: (M+H)⁺ Calc. for C₂₁H₂₃N₂O₂Pt: 530.1, found: 530.2. Anal. Calc. for C₂₁H₂₂N₂O₂Pt: C, 47.64; H, 4.19; N, 5.29. Found: C, 47.84; H, 4.27; N, 5.19%.

3.4. Structure determination

Crystals of **3c** and **3d** were obtained by recrystallization from CH₂Cl₂-methanol at room temperature. Crystallographic data for **3c** were collected at 291(2) K on a Bruker

APEX-II area-detector diffractometer with Mo K α radiation ($\lambda = 0.71073 \text{ \AA}$). Absorption corrections were applied by using SADABS. The hydrogen atoms were assigned with common isotropic displacement factors and included in the final refinement by using geometrical restraints. Crystallographic data for **3d** were measured on a Rigaku-Raxis-IV X-ray diffractometer using graphite-monochromated Mo K α radiation ($\lambda = 0.71073 \text{ \AA}$) at 293(2) K. The hydrogen atoms were included but not refined. The full-matrix least-squares calculations on F^2 were applied on the final refinement. The two structures were solved by direct methods. All non-hydrogen atoms were described anisotropically. Their raw data were corrected and the structures were solved using the SHELX-97 program.

Acknowledgements

We are grateful to the Innovation Fund for Outstanding Scholar of Henan Province (0621001100) and the Natural Science Foundation of Henan Province (0611012100) for financial support of this work.

Appendix A. Supplementary data

CCDC 627418 and 627419 contain the supplementary crystallographic data for **3c** and **3d**. These data can be obtained free of charge via <http://www.ccdc.cam.ac.uk/conts/retrieving.html>, or from the Cambridge Crystallographic Data Centre, 12 Union Road, Cambridge CB2 1EZ, UK; fax: (+44) 1223-336-033; or e-mail: deposit@ccdc.cam.ac.uk. Supplementary data associated with this article can be found, in the online version, at [doi:10.1016/j.jorganchem.2007.01.033](https://doi.org/10.1016/j.jorganchem.2007.01.033).

References

- [1] B. Ma, P.I. Djurovich, M.E. Thompson, *Coord. Chem. Rev.* 249 (2005) 1501, and references cited therein.
- [2] (a) J. Brooks, Y. Babayan, S. Lamansky, P.I. Djurovich, I. Tsyba, R. Bau, M.E. Thompson, *Inorg. Chem.* 41 (2002) 3055;
(b) B. Yin, F. Niemeyer, J.A.G. Williams, J. Jiang, A. Boucekkine, L. Toupet, H. Le Bozec, V. Guerschais, *Inorg. Chem.* 45 (2006) 8584;
(c) N.M. Shavaleev, H. Adams, J. Best, R. Edge, S. Navaratnam, J.A. Weinstein, *Inorg. Chem.* 45 (2006) 9410;
(d) J. Liu, Y. Liu, C. Luo, E. Liu, Y. Yang, Q. Gan, M. Zhu, W. Zhu, *Chem. J. Chin. Univ.* 10 (2006) 1873.
- [3] (a) W. Lu, B.X. Mi, M.C.W. Chan, Z. Hui, N. Zhu, S.T. Lee, C.M. Che, *Chem. Commun.* (2002) 206;
(b) W. Lu, M.C.W. Chan, N. Zhu, C.M. Che, C. Li, Z. Hui, *J. Am. Chem. Soc.* 126 (2004) 7639;
(c) W. Lu, B.X. Mi, M.C.W. Chan, Z. Hui, C.M. Che, N. Zhu, S.T. Lee, *J. Am. Chem. Soc.* 126 (2004) 4958.
- [4] (a) J.A.G. Williams, A. Beeby, E.S. Davies, J.A. Weinstein, C. Wilson, *Inorg. Chem.* 42 (2003) 8609;
(b) W. Sotoyama, T. Satoh, N. Sawatari, H. Inoue, *Appl. Phys. Lett.* 86 (2005) 153505/1;
(c) S.J. Farley, D.L. Rochester, A.L. Thompson, J.A.K. Howard, J.A.G. Williams, *Inorg. Chem.* 44 (2005) 9690.
- [5] (a) Selected examples: B.K.W. Chiu, M.H.W. Lam, D.Y.K. Lee, W.Y. Wong, *J. Organomet. Chem.* 689 (2004) 2888;
(b) T. Kanbara, K. Okada, T. Yamamoto, H. Ogawa, T. Inoue, *J. Organomet. Chem.* 689 (2004) 1860;
(c) G.L. Zhang, Y.T. Chuai, H.Q. Guo, D.C. Zou, *Acta Phys. Chim. Sin.* 21 (2005) 1407;
(d) L. Mao, T. Moriuchi, H. Sakurai, H. Fujii, T. Hirao, *Tetrahedron Lett.* 46 (2005) 8419;
(e) K. Okamoto, T. Kanbara, T. Yamamoto, A. Wada, *Organometallics* 25 (2006) 4026.
- [6] (a) C. Navarro-Ranninger, F. Zamora, I. López-Solera, A. Monge, J.R. Masaguer, *J. Organomet. Chem.* 506 (1996) 149;
(b) F. Zamora, V.M. González, J.M. Pérez, J.R. Masaguer, C. Alonso, C. Navarro-Ranninger, *Appl. Organomet. Chem.* 11 (1997) 659.
- [7] N.A. Boland, M. Casey, S.J. Hynes, J.W. Matthews, M.P. Smyth, *J. Org. Chem.* 67 (2002) 3919.
- [8] X.Q. Hao, J.F. Gong, C.X. Du, L.Y. Wu, Y.J. Wu, M.P. Song, *Tetrahedron Lett.* 47 (2006) 5033.
- [9] T. Kanbara, T. Yamamoto, *J. Organomet. Chem.* 688 (2003) 15.
- [10] C. Janiak, *J. Chem. Soc., Dalton Trans.* (2000) 3885.
- [11] S.R. Meech, D. Phillips, *J. Photochem.* 23 (1983) 193.
- [12] X.C. Liao, X.L. Wu, W.Z. Wang, *Zhengzhou Daxue Xuebao, Lixueban* 34 (2002) 92.
- [13] P. Dash, D.P. Kudav, J.A. Parihar, *J. Chem. Res.* (2004) 490.